

Spectral Energy Distributions and Age Estimates of 78 Star Clusters in M33

Jun Ma¹, Xu Zhou¹, Jiansheng Chen¹, Hong Wu¹, Zhaoji Jiang¹, Suijian Xue¹, and Jin Zhu¹,

Received _____; accepted _____

arXiv:astro-ph/0202363v1 20 Feb 2002

¹National Astronomical Observatories, Chinese Academy of Sciences, Beijing, 100012, P. R. China;
majun@vega.bac.pku.edu.cn

ABSTRACT

In this third paper of our series, we present CCD spectrophotometry of 78 star clusters that were detected by Chandar, Bianchi, & Ford in the nearby spiral galaxy M33. CCD images of M33 were obtained as a part of the BATC Color Survey of the sky in 13 intermediate-band filters from 3800 to 10000Å. By aperture photometry, we obtain the spectral energy distributions of these 78 star clusters. As Chandar, Bianchi, & Ford did, we estimate the ages of our sample clusters by comparing the photometry of each object with theoretical stellar population synthesis models for different values of metallicity. We find that the sample clusters formed continuously in M33 from $\sim 3 \times 10^6 - 10^{10}$ years. This conclusion is consistent with Chandar, Bianchi, & Ford. The results also show that, there are two peaks in cluster formation, at $\sim 8 \times 10^6$ and $\sim 10^9$ years in these clusters.

Subject headings: galaxies: individual (M33) – galaxies: evolution – galaxies: star clusters

1. INTRODUCTION

The importance of the study of star clusters is difficult to overstate, especially in Local Group galaxies. Star clusters, which represent, in distinct and luminous “packets”, single age and single abundance points, and encapsulate at least a partial history of the parent galaxy’s evolution, can provide a unique laboratory for studying. For example, globular clusters can be utilized to provide a lower limit to the age of the parent galaxy provided their ages can be ascertained, and to study the properties of the parent galaxy soon after its formation.

M33 is a small Scd Local Group galaxy, about 15 times farther from us than the LMC (distance modulus is 24.64) (Freedman, Wilson, & Madore 1991; Chandar, Bianchi, & Ford 1999a). It is interesting and important because it represents a morphological type intermediate between the largest “early-type” spirals and the dwarf irregulars in the Local Group (Chandar, Bianchi, & Ford 1999a). Besides, At a distance of ~ 840 kpc, M33 is the only nearby late-type spiral galaxy, it can provide an important link between the cluster populations of earlier-type spirals (Milky Way galaxy and M31) and the numerous, nearby later-type dwarf galaxies. A database of star clusters for M33 have been yielded from the ground-based work (Hiltner 1960; Kron & Mayall 1960; Christian & Schommer 1982, 1988; Melnick & D’Odorico 1978; Mochejska et al. 1998), and from the *Hubble Space Telescope (HST)* images (Chandar, Bianchi, & Ford 1999a; Chandar, Bianchi, & Ford 2001). Especially, the *HST* spatial resolution allowed Chandar, Bianchi, & Ford (1999a, 2001) to penetrate the crowded, spiral regions of M33, yielding the unbiased, representative sample of star clusters, which can be used to probe the global properties of M33. Since clusters at the distance of M33 are easily distinguished from stellar sources in *HST* WFPC2 images, the clusters detected by *HST* WFPC2 images are reliable.

Using the *Hubble Space Telescope* WFPC2 multiband images of 20 fields in M33, Chandar, Bianchi, & Ford (1999a) detected 60 star clusters in this spiral galaxy. These clusters sample a variety of environments from outer regions to spiral arms and central regions, and are the first unbiased, representative sample of star clusters in M33. Then, Chandar, Bianchi, & Ford (1999b) estimated the ages and masses for these star clusters by comparing the integrated photometric measurements with evolutionary models and theoretical M/L_V ratios. They found the 60 star clusters to form continuously in their parent galaxy from $\sim 4 \times 10^6 - 10^{10}$ years, and to have masses between $\sim 4 \times 10^2$ and $3 \times 10^5 M_\odot$.

M33 was observed as part of galaxy calibration program of the Beijing-Arizona-Taiwan-Connecticut (BATC) Multicolor Sky Survey (Fan et al. 1996; Zheng et al. 1999) from September 23, 1995. This program uses the 60/90 cm Schmidt telescope at the Xinglong Station of Beijing Astronomical Observatory (BAO), and has custom designed a set of 15 intermediate-band filters to do spectrophotometry for preselected 1 deg² regions of the northern sky. The BAO Schmidt telescope is equipped with a Ford 2048 \times 2048 Ford CCD at its main focus. Using the 13 intermediate-band filters images of M33 obtained from the BATC

Multicolor Sky Survey, Ma et al. (2001) studied the 60 star clusters of Chandar et al. (1999a). They (Ma et al. 2001) presented the SEDs by aperture photometry, and estimated the ages by comparing the integrated photometric measurements with theoretical stellar population synthesis models for these star clusters. We can provide the accurate SEDs for these star clusters using the multi-color photometry of BATC.

From 35 deep *Hubble Space Telescope (HST)* WFPC2 fields, Chandar, Bianchi, & Ford (2001) again detected 102 star clusters in M33, eighty-two of which had not previously been detected. Using one dereddened color $((V - I)_0)$, they estimated the ages and masses for these clusters with single stellar population models. However, they did not give quantitative age estimates for individual clusters due to the relatively large uncertainty associated with age estimates from comparison of one color with single stellar population models.

In this paper, we present the SEDs of 78 star clusters that were detected by Chandar, Bianchi, & Ford (2001) in M33, and quantitatively estimate the ages for these clusters by comparing the integrated photometric measurements with theoretical stellar population synthesis models.

The outline of the paper is as follows. Details of observations and data reduction are given in section 2. In section 3, we provide a brief description of the stellar population synthesis models of G. Bruzual & S. Charlot (1996, unpublished). The age estimates for the star clusters are given in section 4. The summary and discussion are presented in section 5.

2. SAMPLE OF STAR CLUSTERS, OBSERVATIONS AND DATA REDUCTION

2.1. Sample of Star Clusters

The sample of star clusters in this paper is from Chandar, Bianchi, & Ford (2001), who used 35 deep *Hubble Space Telescope (HST)* WFPC2 fields to extend the search for star clusters in M33, and particularly to focus on detection of older clusters. Since these clusters cover a range of environments from the center to the skirts, they can be used to probe the global properties of the parent galaxy. At the same time, the accurate positions of these star clusters are presented in Chandar, Bianchi, & Ford (2001). So, we select these star clusters to be studied, and obtain their SEDs in the 13 intermediate-band filters by aperture photometry. The age estimates for these star clusters are obtained using the theoretical evolutionary population synthesis methods. Clusters 63, 65, 66, 80, 82, 85, 102, 105, 111, 123, 134, 138, 140, 143 and 149 are not included in our sample because of their low signal-to-noise ratio in the images of some BATC filters. Besides, clusters 61, 70, 81, 90, 98, 104, 106, 114 and 116 are U49, M9, C20, U77, R14, H38, H10, C38 and R12 of Christian & Schommer (1982) respectively, the SEDs and ages of which were presented (Ma et al. 2002), and are also not included in our sample. The position of cluster 85 presented by Chandar et al. (2001) may be wrong, it should be $RA = 01^h33^m14^s28$ decl.= $30^\circ28'22''.9$, and it is U137

of Christian & Schommer (1982) (see details from Ma et al. 2002).

Figure 1 is the image of M33 in filter BATC07 (5785Å), the circles in which indicate the positions of the sample clusters in this paper.

2.2. Observations and Data Reduction

The large field multi-color observations of the spiral galaxy M33 were obtained in the BATC photometric system. The multi-color BATC filter system, which were specifically designed to avoid contamination from the brightest and most variable night sky emission lines, includes 15 intermediate-band filters, covering the total optical wavelength range from 3000 to 10000Å. The images of M33 covering the whole optical body of M33 were accumulated in 13 intermediate band filters with a total exposure time of about 32.75 hours from September 23, 1995 to August 28, 2000. The dome flat-field images were taken by using a diffuse plate in front of the correcting plate of the Schmidt telescope. For flux calibration, the Oke-Gunn primary flux standard stars HD19445, HD84937, BD+262606 and BD+174708 were observed during photometric nights (see details from Yan et al. 1999, Zhou et al. 2001). *Column 6* in Table 1 gives the calibration error, in magnitude, for the standard stars in each filter. The formal errors we obtain for these stars in the 13 BATC filters are $\lesssim 0.02$ mag. This indicates that we can define the standard BATC system to an accuracy of $\lesssim 0.02$ mag.

The data were reduced with standard procedures, including bias subtraction and flat-fielding of the CCD images, with an automatic data reduction software named PIPELINE I developed for the BATC multi-color sky survey (see Ma et al. 2001, 2002 for a detail).

2.3. Integrated Photometry

For each star cluster, the PHOT routine in DAOPHOT (Stetson 1987, 1992) is used to obtain magnitudes. For avoiding contamination from nearby objects, a smaller aperture of $6''/8$, which corresponds to a diameter of 4 pixels in Ford CCDs, is adopted. Aperture corrections are computed using isolated stars. The spectral energy distributions (SEDs) in 13 BATC filters for 78 star clusters were obtained. Table 2 contains the following information: *Column 1* is cluster number which is taken from Chandar, Bianchi, & Ford (2001). *Column 2* to *Column 14* show the magnitudes of different bands. Second line of each star cluster is the uncertainties of magnitude of corresponding band. The uncertainties for each filter are given by DAOPHOT.

2.4. Comparison with Previous Photometry

Using the Landolt standards, Zhou et al. (2001) presented the relationships between the BATC intermediate-band system and *UBVRI* broadband system by the catalogs of Landolt (1983, 1992) and Galadí-Enríquez et al. (2000). We show the coefficients of one relationship in equation (1).

$$m_V = m_{07} + (0.3233 \pm 0.019)(m_{06} - m_{08}) + 0.0590 \pm 0.010. \quad (1)$$

Using equation (1), we transformed the magnitudes of 78 star clusters in BATC06, BATC07 and BATC08 bands to ones in V band. Figure 2 plots the comparison of *V* (BATC) photometry with previously published measurements (Chandar, Bianchi, & Ford 2001). Table 3 shows this comparison. The mean *V* magnitude difference (this paper’s values minus the values of Chandar et al. 2001) is $\langle \Delta V \rangle = 0.036 \pm 0.042$. The uncertainties in *V* (BATC) have been added linearly, i.e. $\sigma_B = \sigma_{07} + 0.3233(\sigma_{06} + \sigma_{08})$, to reflect the error in the three filter measurements. From Figure 2 and Table 3, it can be seen that there is good agreement in the photometric measurements between Chandar, Bianchi, & Ford (2001) and this paper except for clusters 115 and 127.

3. DATABASES OF SIMPLE STELLAR POPULATIONS

Tinsley (1972) and Searle et al. (1973) did the pioneering work in evolutionary population synthesis. This method has become a standard technique to study the stellar populations of galaxies. This is a result of the improvement in the theory of the chemical evolution of galaxies, star formation, stellar evolution and atmospheres, and of the development of synthesis algorithms and the availability of various evolutionary synthesis models. A comprehensive compilation of such models was presented by Leitherer et al. (1996) and Kennicutt (1998). More widely used models are from the Padova and Geneva group (e.g. Schaerer & de Koter 1997; Schaerer & Vacca 1998; Bressan et al. 1996; Chiosi et al. 1998), GISSEL96 (Charlot & Bruzual 1991; Bruzual & Charlot 1993; G. Bruzual & S. Charlot 1996, unpublished), PEGASE (Fioc & Rocca-Volmerange 1997) and STARBURST99 (Leitherer et al. 1999).

A simple stellar population (SSP) is defined as a single generation of coeval stars with fixed parameters such as metallicity, initial mass function, etc. (Buzzoni 1997). SSPs are the basic building blocks of synthetic spectra of galaxies that can be used to infer the formation and subsequent evolution of the parent galaxies (Jablonka et al. 1996). They are modeled by a collection of stellar evolutionary tracks with different masses and initial chemical compositions, supplemented with a library of stellar spectra for stars at different evolutionary stages in evolution synthesis models. In this paper, we use the SSPs of Galaxy Isochrone Synthesis Spectra Evolution Library (hereafter GSSP; G. Bruzual & S. Charlot 1996, unpublished) to estimate the ages of the sample clusters, since they are simple and reasonably well understood.

3.1. Spectral Energy Distribution of GSSPs

Charlot & Bruzual (1991) developed a model of stellar population synthesis. In this model, the population synthesis method can be used to determine the distribution of stars in the theoretical color-magnitude diagram (CMD) for any stellar system. Bruzual & Charlot (1993) presented “isochrone synthesis” as a natural and reliable approach to model the evolution of stellar populations in star clusters and galaxies. With this isochrone synthesis algorithm, Bruzual & Charlot (1993) computed the spectral energy distributions of stellar populations with solar metallicity. G. Bruzual & S. Charlot (1996, unpublished) improved the Bruzual & Charlot (1993) evolutionary population synthesis models. The updated version provides the evolution of the spectrophotometric properties for a wide range of stellar metallicity, which are $Z = 0.0004, 0.004, 0.008, 0.02, 0.05,$ and 0.1 (see Ma et al. 2001, 2002 for a detail).

3.2. Integrated Colors of GSSPs

Kong et al. (2000) have obtained the age, metallicity, and interstellar-medium reddening distribution for M81. They found the best match between the intrinsic colors and the predictions of GSSP for each cell of M81. To estimate the ages for the sample clusters in this paper, we follow the method of Kong et al. (2000). As we know, the observational data are integrated luminosity. So, we need to convolve the SED of GSSP with BATC filter profiles to obtain the optical and near-infrared integrated luminosity for comparisons (Kong et al. 2000). The integrated luminosity $L_{\lambda_i}(t, Z)$ of the i th BATC filter can be calculated with

$$L_{\lambda_i}(t, Z) = \frac{\int F_{\lambda}(t, Z)\varphi_i(\lambda)d\lambda}{\int \varphi_i(\lambda)d\lambda}, \quad (2)$$

where $F_{\lambda}(t, Z)$ is the spectral energy distribution of the GSSP of metallicity Z at age t , $\varphi_i(\lambda)$ is the response functions of the i th filter of the BATC filter system ($i = 3, 4, \dots, 15$), respectively. For avoiding to use the parameters that are dependent on the distance. We calculate the integrated colors of a GSSP relative to the BATC filter BATC08 ($\lambda = 6075\text{\AA}$):

$$C_{\lambda_i}(t, Z) = L_{\lambda_i}(t, Z)/L_{6075}(t, Z). \quad (3)$$

As a result, we obtained the intermediate-band colors of a GSSP for 6 metallicities from $Z=0.0004$ to $Z=0.1$ using equations (2) and (3).

4. AGE ESTIMATES

In order to obtain intrinsic colors of 78 clusters and hence accurate ages, the photometric measurements must be dereddened. As Chandar, Bianchi, & Ford (2001) did, we adopted $E(B - V) = 0.10$. Besides, we

adopted the extinction curve presented by Zombeck (1990). An extinction correction $A_\lambda = R_\lambda E(B - V)$ was applied, here R_λ is obtained by interpolating using the data of Zombeck (1990).

Since we model the stellar populations of the star clusters by SSPs, the intrinsic colors for each star cluster are determined by two parameters: age, and metallicity. We will determine the ages and best-fitted models of metallicity for these star clusters simultaneously by a least square method. The age and best-fitted model of metallicity are found by minimizing the difference between the intrinsic and integrated colors of GSSP:

$$R^2(n, t, Z) = \sum_{i=3}^{15} [C_{\lambda_i}^{\text{intr}}(n) - C_{\lambda_i}^{\text{ssp}}(t, Z)]^2, \quad (4)$$

where $C_{\lambda_i}^{\text{ssp}}(t, Z)$ represents the integrated color in the i th filter of a SSP at age t in the model of metallicity Z , and $C_{\lambda_i}^{\text{intr}}(n)$ is the intrinsic integrated color for n th star cluster. Using the stellar evolutionary models (Bertelli et al. 1994) and published line indices of 22 M33 older clusters, Chandar, Bianchi, & Ford (1999b) narrowed the range of cluster metallicities (Z) to be from ~ 0.0002 to 0.03 . So, we only select the models of three metallicities, 0.0004 , 0.004 and 0.02 of GSSP.

Figure 3 shows the map of the best fit of the integrated color of a SSP with the intrinsic integrated color for 78 star clusters, and Table 4 presents the best-fitted models of metallicities and ages for these star clusters. In Figure 3, the thick line represents the integrated color of a SSP of GSSP, and filled circle represents the intrinsic integrated color of a star cluster. From this figure, we see that clusters 83, 88 and 148 have strong emission lines. In the process of fitting, we did not use the strong emission lines.

Figure 4 presents a histogram of cluster ages. The results show that, in general, M33 clusters have been forming continuously, with ages of $\sim 3 \times 10^6 - 10^{10}$ years. This conclusion confirms the results of Chandar, Bianchi, & Fort (2001). There exist three groups of clusters that formed with three models of metallicities, $Z = 0.02, 0.004$, and 0.0004 . In different models of metallicities, the distribution of cluster ages is a little different, too. In the model of $Z = 0.02$, the ages of most clusters are younger than $\sim 10^9$ years, and there are two peaks at $\sim 10^7$ and $\sim 10^9$ years. In the model of $Z = 0.004$, the clusters formed from $\sim 3 \times 10^6 - 10^{10}$ years, and the distribution of ages is more homogeneous than in the other two models. In the model of $Z = 0.0004$, the most clusters formed from $\sim 10^8 - 10^{10}$ years. Clusters 97, 106 and 162 have derived ages consistent with that of the globular clusters of the Milky Way, $\sim 1.5 \times 10^{10}$ years. This result is also consistent with that found by Chandar, Bianchi, & Fort (1999b) and Ma et al. (2001), who presented clusters 11, 28, 29 and 57 to be as old as $\sim 1.5 \times 10^{10}$ years.

In this section, we estimate the ages of our sample clusters by comparing the photometry of each object with the theoretical stellar population synthesis models for different values of metallicity. However, we want to emphasize that, for clusters older than several 10^8 years, the age/metallicity degeneracy becomes

pronounced. In this case, we only mean that in some model of metallicity, the intrinsic integrated color of a cluster can do the best fit with the integrated color of a SSP at some age. Besides, the uncertainties in the age estimates arising from photometric uncertainties are 0.2 or so, i.e, $\text{age} \pm 0.2 \times \text{age}$ [log yr].

5. SUMMARY AND DISCUSSION

In this paper, we have, for the first time, obtained the SEDs of 78 star clusters of M33 in 13 intermediate colors with the BAO 60/90 cm Schmidt telescope. Below, we summarize our main conclusions.

1. Using the images obtained with the Beijing Astronomical Observatory 60/90 cm Schmidt Telescope in 13 intermediate-band filters from 3800 to 10000Å, we obtained the spectral energy distributions (SEDs) of 78 star clusters that were detected by Chandar, Bianchi, & Ford (2001).

2. By comparing the integrated photometric measurements with theoretical stellar population synthesis models, we find that clusters formed continuously in M33 from $\sim 3 \times 10^6 - 10^{10}$ years. The results also show that, there are two peaks at $\sim 8 \times 10^6$ and $\sim 10^9$ years.

Chandar et al. (1999a, 1999b) estimated ages for 60 star clusters in M33 by comparing the photometric measurements to integrated color from theoretical models by Bertelli et al. (1994). Their results showed that, the integrated colors of star clusters depend mostly on age, with a secondary dependence on chemical composition. So, we can estimate ages of clusters, but cannot determine metallicities of clusters exactly. As Chandar, Bianchi, & Ford (1999b, 1999c, 2001) did, we also estimated the ages of our sample clusters by comparing the photometry of each object with models for different values of metallicity. Although we presented the metallicity of each cluster in Table 4, we only mean that, in this model of metallicity, the intrinsic integrated color of each cluster can do the best fit with the integrated color of a SSP.

With spectrophotometry, Christian & Schommer (1983) obtained the ages of the star clusters in M33 to be $\sim 10^7 - 10^{10}$ years. Using the integrated *UBV* photometry and IUE $\lambda\lambda 1200 - 3000$ Å spectra, Ciani, D’Odorico, & Benvenuti (1984) studied the minuscule “bulge” population of M33 and found that, a multigeneration model, where a young component (age $\sim 10^7$ years) and an old, metal-poor one (age $\sim 5 \times 10^9$ years) are superposed, gives the best fit to the observed data. Schmidt, Bica, & Alloin (1990) applied a population synthesis method which uses a star cluster spectral library and a grid of the star cluster spectral properties as a function of age and metallicity (Bica & Alloin 1986a, b; 1987), to the blueish nucleus of M33, and gave an age of less than 5×10^8 years for the dominant blue bulge population. From the histogram of ages in this paper, we can see that some old clusters in our sample appear to be coeval with the old population of the bulge.

improved this paper. We are grateful to the Padova group for providing us with a set of theoretical isochrones and SSPs. We also thank G. Bruzual and S. Charlot for sending us their latest calculations of SSPs and for explanations of their code. The work is supported partly by the National Sciences Foundation under the contract No.19833020 and No.19503003. The BATC Survey is supported by the Chinese Academy of Sciences, the Chinese National Natural Science Foundation and the Chinese State Committee of Sciences and Technology. The project is also supported in part by the National Science Foundation (grant INT 93-01805) and by Arizona State University, the University of Arizona and Western Connecticut State University.

Fig. 1.— The image of M33 in filter BATC07 (5785\AA) and the positions of the sample star clusters. The image size is $52' \times 53'$. The center of the image is located at RA = $01^{\text{h}}33^{\text{m}}50^{\text{s}}.58$ DEC= $30^{\circ}39'08''.4$ (J2000.0). North is up and east is to the left.

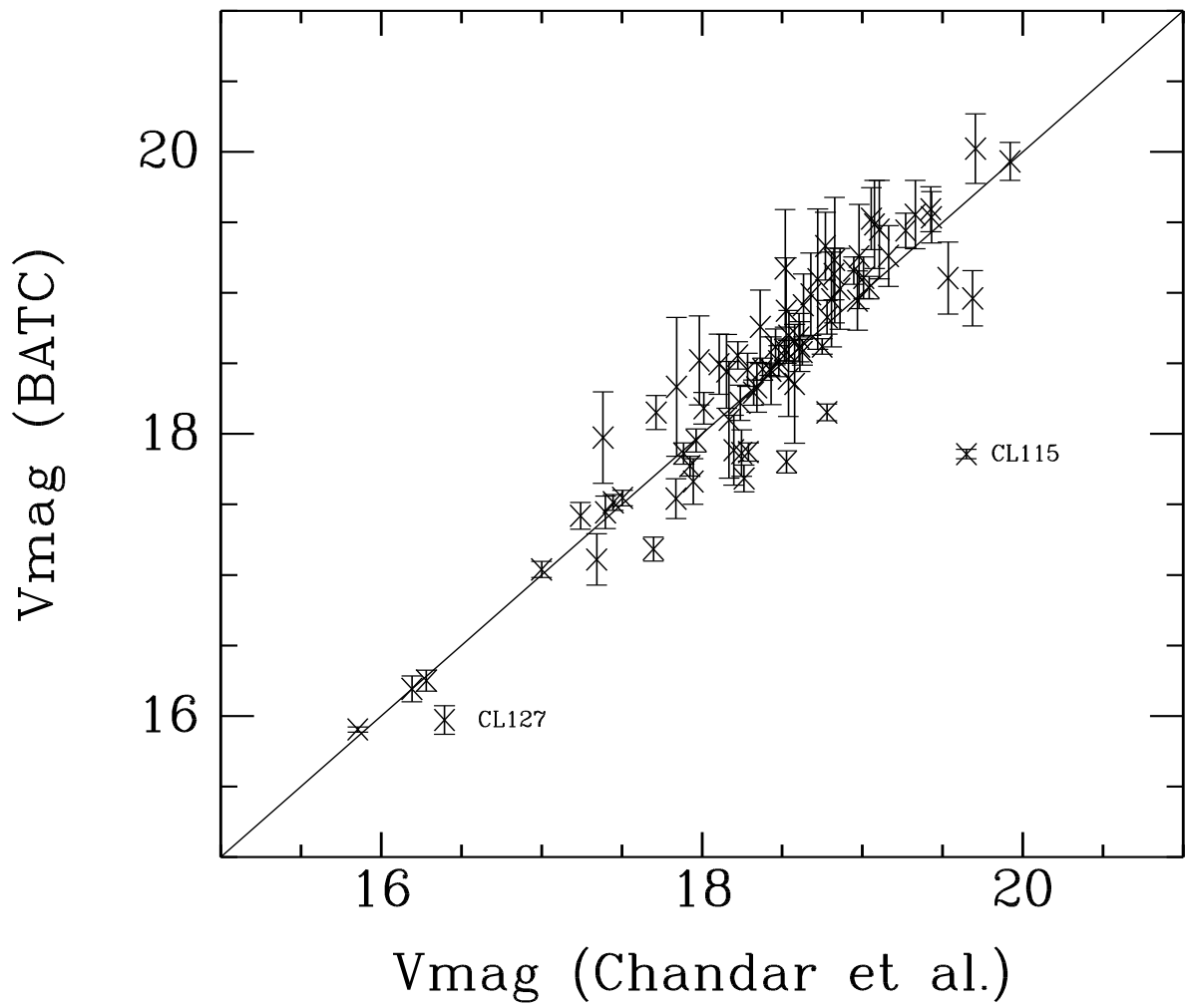


Fig. 2.— Comparison of Cluster Photometry with Previous Measurements (*HST*)

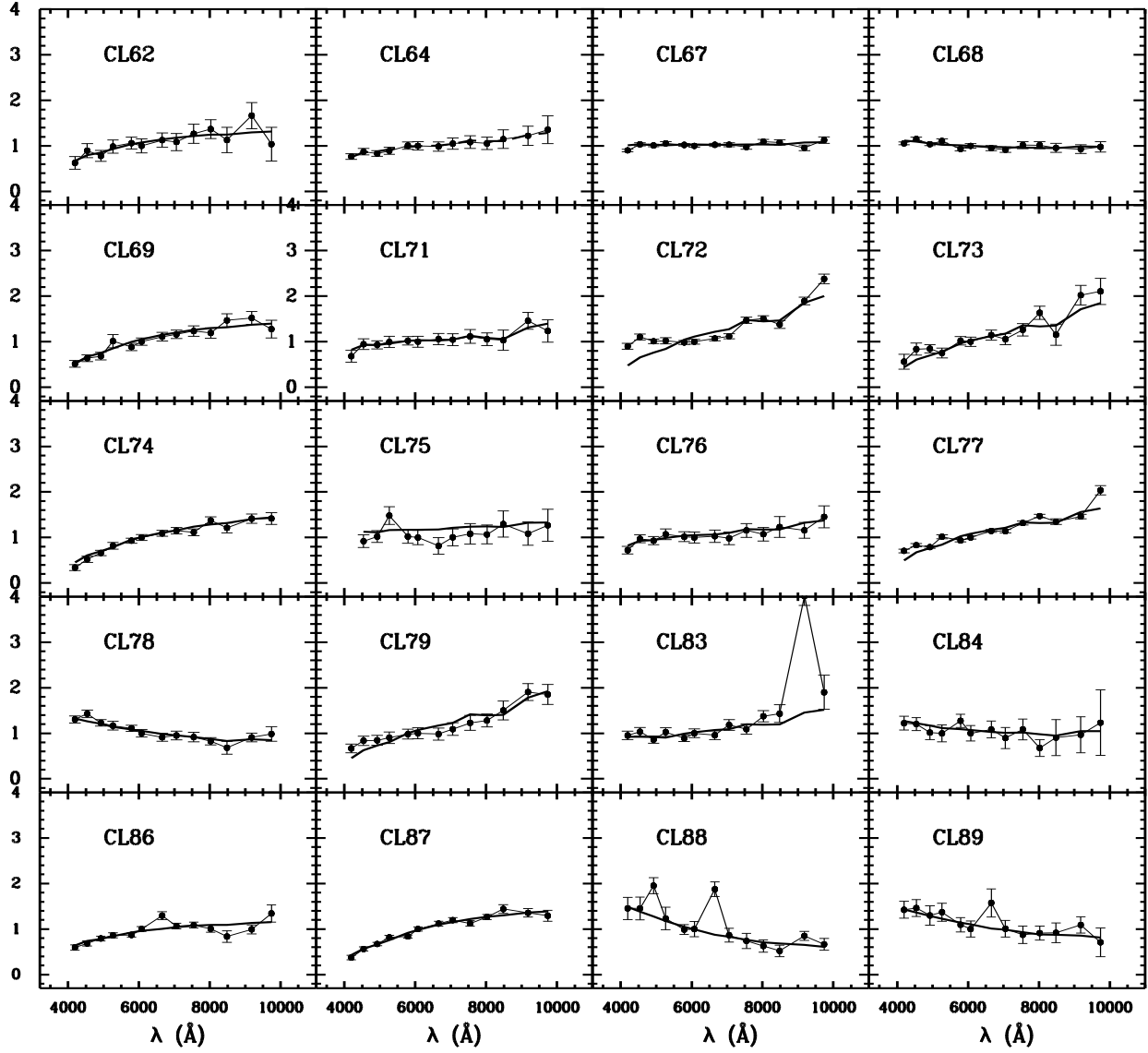


Fig. 3.— Map of the best fit of the integrated color of a SSP with intrinsic integrated color for 78 star clusters. Thick line represents the integrated color of a SSP, and filled circle represents the intrinsic integrated color of a star cluster.

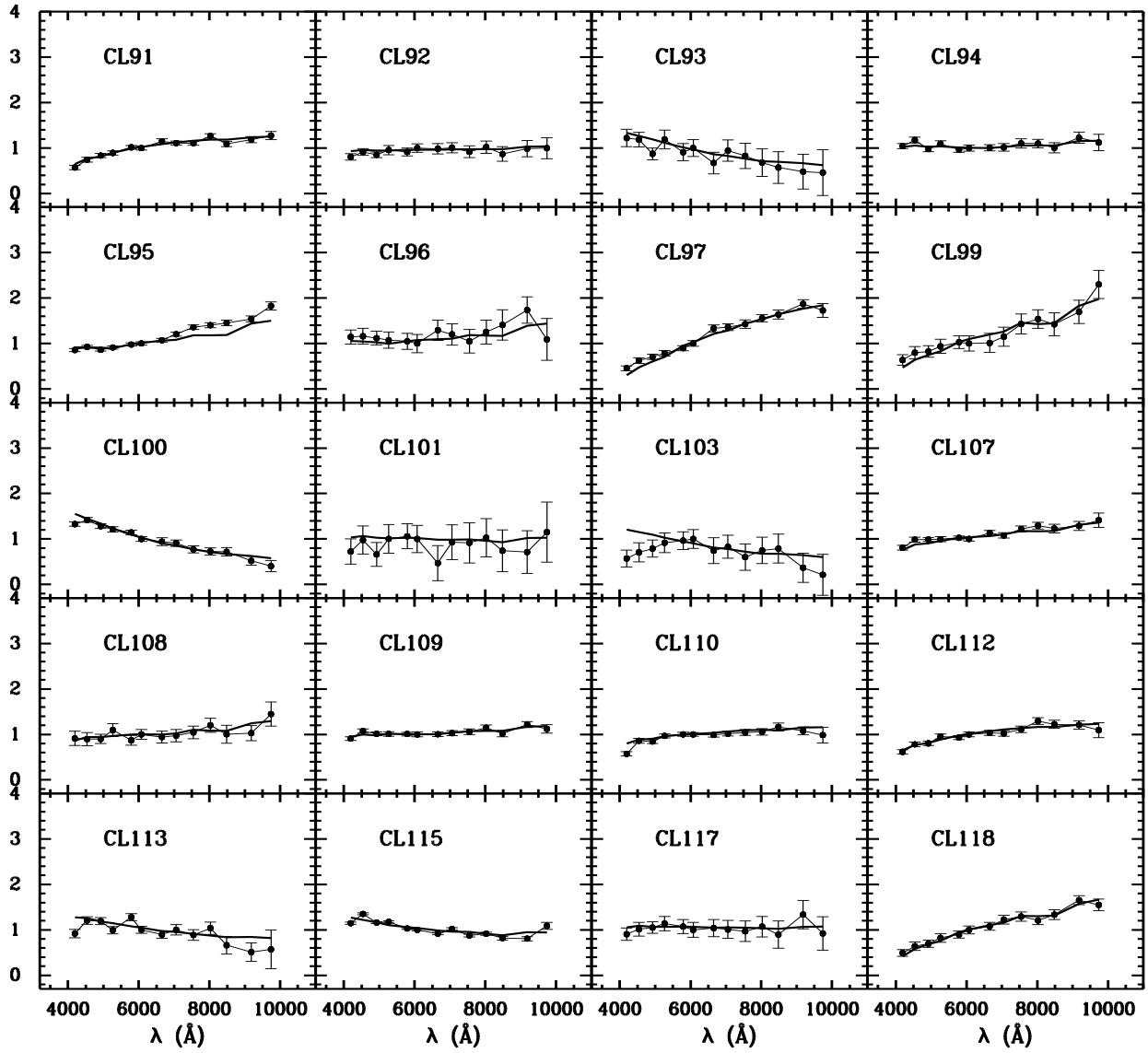


Fig. 3.— Continued

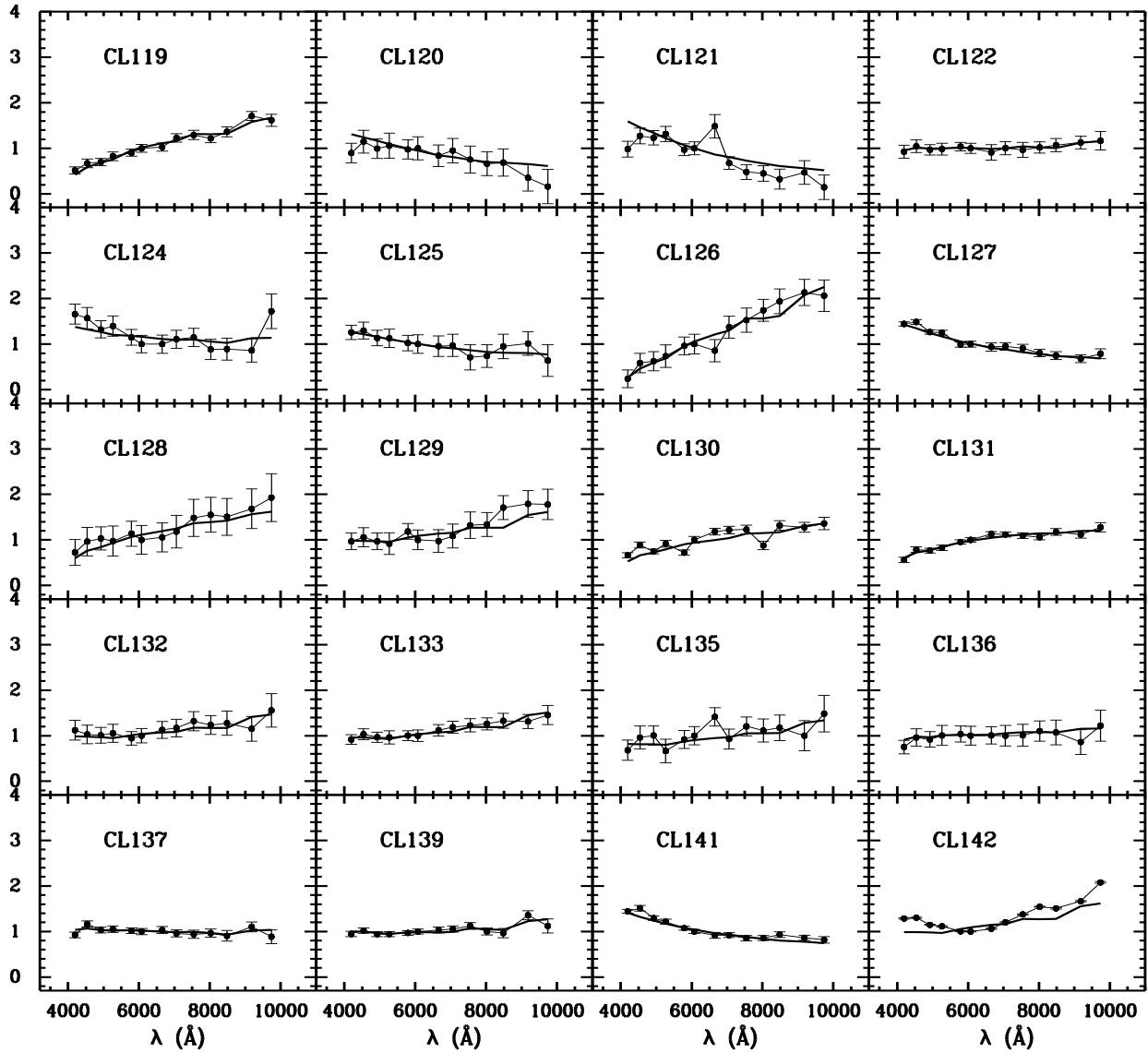


Fig. 3.— Continued

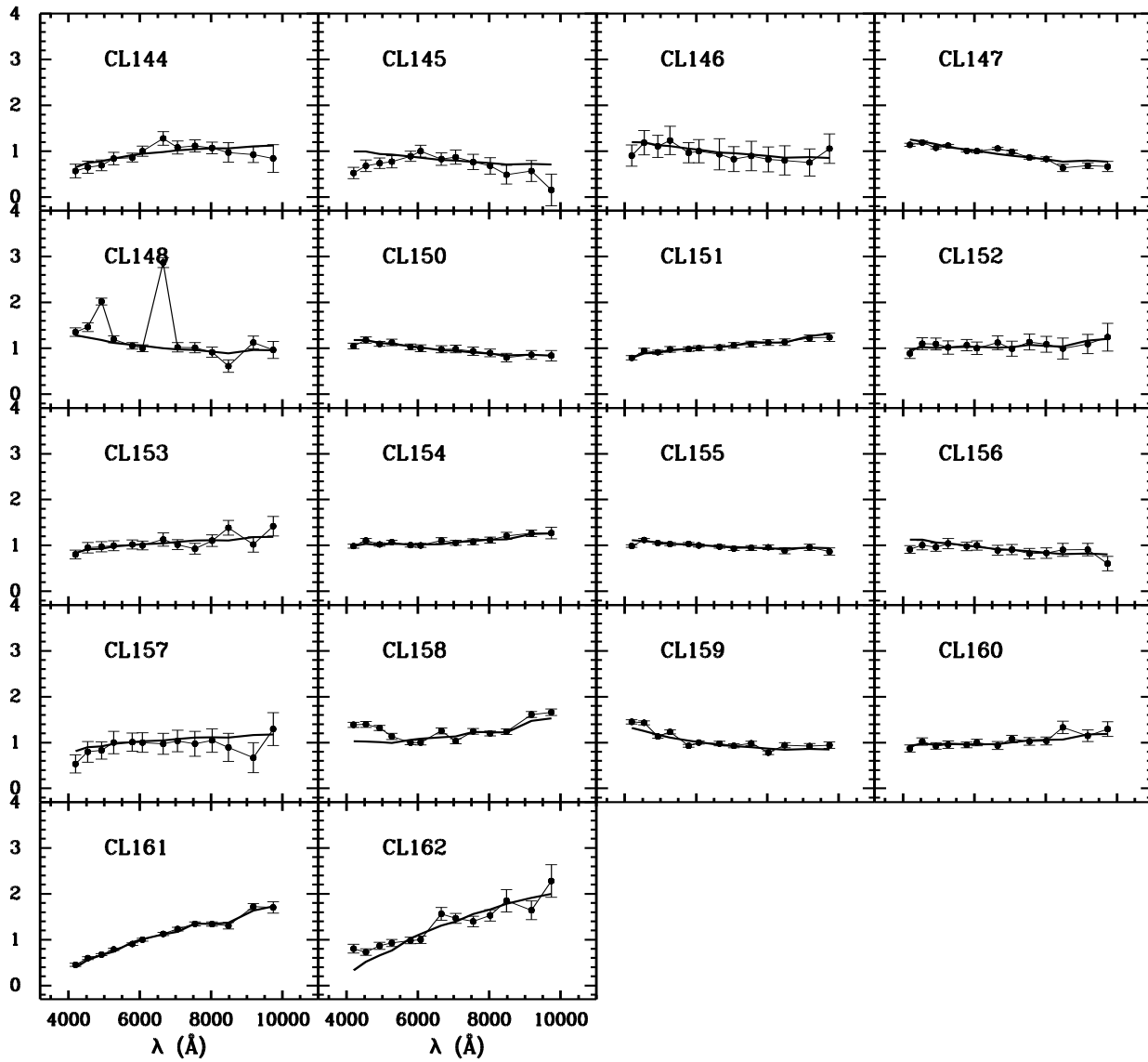


Fig. 3.— Continued

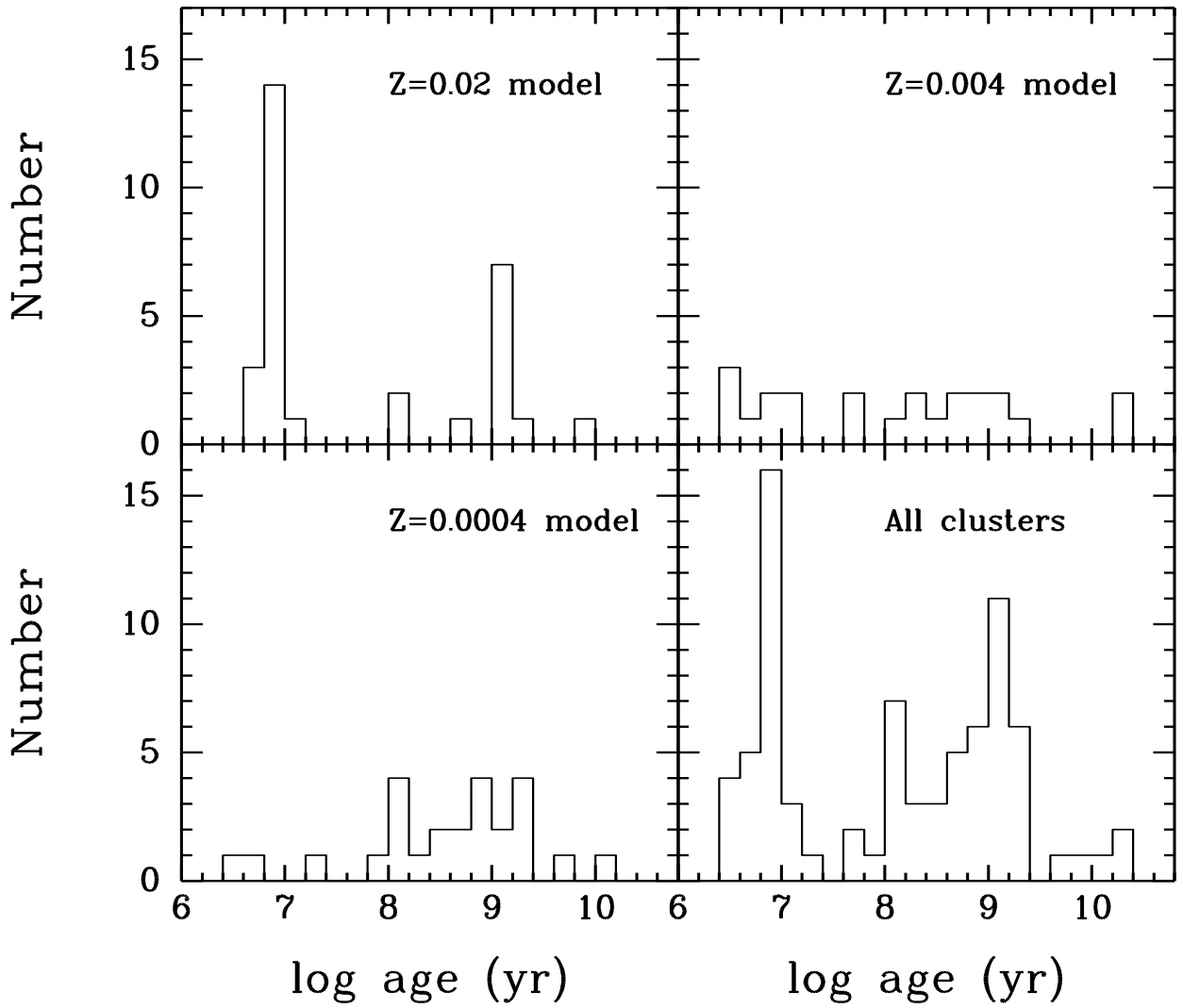


Fig. 4.— Histogram of M33 cluster ages

REFERENCES

- Bertelli, O., Bressan, A., Chiosi, C., Fagotto, F., & Nasi, E. 1994, *A&AS*, 106, 275
- Bica, E., & Alloin, D. 1986a, *A&A*, 162, 21
- Bica, E., & Alloin, D. 1986b, *A&AS*, 66, 171
- Bica, E., & Alloin, D. 1987, *A&A*, 186, 49
- Bressan, A., Chiosi, C., & Tantalo, R. 1996, *A&A*, 311, 425
- Bruzual, G., & Charlot, S. 1993, *ApJ*, 405, 538
- Buzzoni, A. 1997, in *IAU Symp. 183, Cosmological Parameters and Evolution of the Universe*, ed. K. Sato, 18
- Chandar, R., Bianchi, L., & Ford, H. C. 1999a, *ApJS*, 122, 431
- Chandar, R., Bianchi, L., & Ford, H. C. 1999b, *ApJ*, 517, 668
- Chandar, R., Bianchi, L., Ford, H. C., & Salasnich, B. 1999c, *PASP*, 111, 794
- Chandar, R., Bianchi, L., & Ford, H. C. 2001, *A&A*, 366, 498
- Charlot, S., & Bruzual, G. 1991, *ApJ*, 367, 126
- Chiosi, C., Bressan, A., Portinari, L., & Tantalo, R. 1998, *A&A*, 339, 355
- Christian, C. A., & Schommer, R. A. 1982, *ApJS*, 49, 405
- Christian, C. A., & Schommer, R. A. 1983, *ApJ*, 275, 92
- Christian, C. A., & Schommer, R. A. 1988, *AJ*, 95, 704
- Ciani, A., D’Odorico, S., & Benvenuti, P. 1984, *A&A*, 137, 223
- Fan, X.-H., et al. 1996, *AJ*, 112, 628
- Fioc, M., & Rocca-Volmerange, B. 1997, *A&A*, 326,950
- Freedman, W. L., Wilson, C. D., & Madore, B. F. 1991, *ApJ*, 372, 455
- Galadí-Enríquez, D., Trullols, E., & Jordi, C. 2000, *A&AS*, 146, 169
- Hiltner, W. A. 1960, *ApJ*, 131, 163

- Jablonka, P., Bica, E., Pelat, D., & Alloin, D. 1996, *A&A*, 307, 385
- Kennicutt, R. C. 1998, *ARA&A*, 36, 189
- Kong, X., et al. 2000, *AJ*, 119, 2745
- Kron, G. E., & Mayall, N. U. 1960, *AJ*, 65, 581
- Landolt, A. U. 1983, *AJ*, 88, 439
- Landolt, A. U. 1992, *AJ*, 104, 340
- Leitherer, C., et al. 1996, *PASP*, 108, 996
- Leitherer, C., et al. 1999, *ApJS*, 123, 3
- Ma, J., et al. 2001, *AJ*, 122, 1796
- Ma, J., et al. 2002, *A&A*, in press
- Melnick, J., & D’Odorico, S. 1978, *A&AS*, 34, 249
- Mochejska, B. J., Kaluzny, J., Krockenberger, M., Sasselov, D. D., & Stanek, K. Z. 1998, *Acta Astron.*, 48, 455
- Schaerer, D., & de Koter, A. 1997, *A&A*, 322, 598
- Schaerer, D., & Vacca, W. D. 1998, *ApJ*, 497, 618
- Schmidt, A. A., Bica, E., & Alloin, D. 1990, *MNRAS*, 243, 620
- Searle, L., Sargent, W. L. W., & Bagnuolo, W. G. 1973, *ApJ*, 179, 427
- Stetson, P. B. 1987, *PASP*, 99, 191
- Stetson, P. B. 1992, *PASP*, 25, 297
- Tinsley, B. M. 1972, *A&A*, 20, 383
- Yan, H. J., et al. 2000, *PASP*, 112, 691
- Zheng, Z. Y., et al. 1999, *AJ*, 117, 2757
- Zhou, X., et al. 2001, *CJAA*, 1, 372
- Zhou, X., et al. 2001, submitted

Zombeck, M. V. 1990, Handbook of Space Astronomy and Astrophysics (2nd. ed; Cambridge: Cambridge Univ. Press)

Table 1: Parameters of the BATC Filters and Statistics of Observations

No.	Name	cw ^a (Å)	Exp. (hr)	N.img ^b	rms ^c
1	BATC03	4210	00:55	04	0.024
2	BATC04	4546	01:05	04	0.023
3	BATC05	4872	03:55	19	0.017
4	BATC06	5250	03:19	15	0.006
5	BATC07	5785	04:38	17	0.011
6	BATC08	6075	01:26	08	0.016
7	BATC09	6710	01:09	08	0.006
8	BATC10	7010	01:41	08	0.005
9	BATC11	7530	02:07	10	0.017
10	BATC12	8000	03:00	11	0.003
11	BATC13	8510	03:15	11	0.005
12	BATC14	9170	01:15	05	0.011
13	BATC15	9720	05:00	26	0.009

^aCentral wavelength for each BATC filter

^bImage numbers for each BATC filter

^cCalibration error, in magnitude, for each filter as obtained from the standard stars

Table 2: SEDs of 78 Star Clusters

No.	03	04	05	06	07	08	09	10	11	12	13	14
(1)	(2)	(3)	(4)	(5)	(6)	(7)	(8)	(9)	(10)	(11)	(12)	(13)
62	19.970	19.551	19.672	19.377	19.248	19.301	19.142	19.172	18.984	18.881	19.070	18.627
	0.238	0.186	0.168	0.162	0.133	0.168	0.151	0.188	0.180	0.166	0.268	0.187
64	19.433	19.262	19.282	19.171	18.988	18.984	18.969	18.891	18.837	18.848	18.735	18.646
	0.089	0.087	0.082	0.094	0.084	0.100	0.111	0.127	0.137	0.140	0.192	0.187
67	17.742	17.563	17.559	17.470	17.456	17.469	17.414	17.402	17.435	17.293	17.288	17.396
	0.034	0.033	0.032	0.039	0.032	0.034	0.037	0.044	0.052	0.049	0.060	0.068
68	17.925	17.801	17.883	17.773	17.910	17.824	17.849	17.879	17.747	17.729	17.774	17.784
	0.032	0.036	0.035	0.043	0.051	0.052	0.066	0.071	0.083	0.084	0.113	0.115
69	19.363	19.100	18.992	18.525	18.623	18.478	18.336	18.276	18.191	18.208	17.961	17.903
	0.154	0.125	0.135	0.155	0.100	0.088	0.093	0.087	0.099	0.103	0.106	0.102
71	19.640	19.258	19.241	19.131	19.054	19.065	18.974	18.977	18.887	18.928	18.931	18.535
	0.205	0.135	0.105	0.134	0.097	0.131	0.125	0.134	0.146	0.145	0.233	0.138
72	18.468	18.216	18.284	18.230	18.222	18.193	18.091	18.031	17.715	17.667	17.745	17.380
	0.080	0.062	0.055	0.070	0.048	0.058	0.052	0.056	0.051	0.046	0.067	0.047
73	20.156	19.692	19.652	19.739	19.357	19.368	19.191	19.269	19.056	18.755	19.113	18.484
	0.319	0.171	0.112	0.155	0.097	0.110	0.104	0.129	0.118	0.097	0.220	0.117
74	19.926	19.425	19.138	18.868	18.678	18.589	18.465	18.399	18.410	18.164	18.281	18.094
	0.201	0.142	0.095	0.100	0.064	0.069	0.064	0.068	0.072	0.061	0.098	0.076
75	19.782	19.400	19.256	18.811	19.164	19.177	19.370	19.133	19.033	19.028	18.796	18.969
	0.190	0.164	0.139	0.143	0.155	0.169	0.246	0.199	0.228	0.211	0.240	0.256
76	19.427	19.077	19.093	18.900	18.906	18.913	18.852	18.893	18.697	18.758	18.588	18.634
	0.127	0.098	0.105	0.122	0.115	0.129	0.145	0.154	0.144	0.151	0.202	0.161
77	18.534	18.327	18.353	18.037	18.080	17.995	17.819	17.816	17.635	17.497	17.572	17.464
	0.061	0.045	0.039	0.046	0.032	0.036	0.030	0.036	0.035	0.028	0.049	0.037
78	18.169	18.041	18.174	18.191	18.196	18.297	18.368	18.312	18.333	18.426	18.613	18.282
	0.065	0.064	0.064	0.090	0.066	0.092	0.100	0.110	0.124	0.104	0.225	0.114
79	19.398	19.123	19.082	18.970	18.831	18.799	18.789	18.665	18.516	18.452	18.258	17.980
	0.153	0.132	0.139	0.152	0.118	0.133	0.148	0.138	0.143	0.120	0.149	0.105

Table 2: Continued

No.	03	04	05	06	07	08	09	10	11	12	13	14
(1)	(2)	(3)	(4)	(5)	(6)	(7)	(8)	(9)	(10)	(11)	(12)	(13)
88	17.608	17.579	17.228	17.690	17.878	17.855	17.143	17.973	18.123	18.281	18.468	17.912
	0.182	0.185	0.098	0.218	0.119	0.181	0.094	0.190	0.244	0.232	0.266	0.128
89	18.292	18.232	18.331	18.232	18.425	18.514	17.991	18.468	18.601	18.534	18.508	18.300
	0.142	0.136	0.177	0.158	0.156	0.190	0.213	0.195	0.238	0.186	0.256	0.179
91	18.517	18.203	18.047	17.933	17.743	17.750	17.569	17.596	17.579	17.416	17.556	17.447
	0.092	0.074	0.060	0.056	0.042	0.045	0.051	0.042	0.046	0.043	0.059	0.062
92	18.876	18.707	18.755	18.590	18.589	18.481	18.469	18.433	18.515	18.378	18.535	18.376
	0.095	0.089	0.079	0.116	0.102	0.098	0.125	0.121	0.154	0.145	0.200	0.197
93	19.262	19.262	19.566	19.190	19.431	19.318	19.722	19.339	19.461	19.659	19.826	19.992
	0.171	0.147	0.162	0.189	0.223	0.203	0.387	0.269	0.363	0.488	0.660	0.867
94	18.533	18.374	18.544	18.382	18.469	18.420	18.382	18.364	18.255	18.239	18.313	18.079
	0.059	0.060	0.064	0.068	0.062	0.076	0.074	0.090	0.099	0.092	0.119	0.109
95	18.055	17.941	17.991	17.887	17.762	17.728	17.622	17.487	17.335	17.280	17.223	17.139
	0.040	0.038	0.036	0.041	0.038	0.041	0.042	0.039	0.041	0.042	0.046	0.045
96	19.486	19.442	19.451	19.457	19.432	19.473	19.164	19.234	19.361	19.148	19.002	18.754
	0.145	0.163	0.147	0.181	0.183	0.219	0.187	0.212	0.269	0.228	0.257	0.181
97	19.183	18.805	18.641	18.486	18.293	18.168	17.825	17.793	17.723	17.607	17.532	17.369
	0.125	0.105	0.091	0.086	0.067	0.068	0.063	0.059	0.069	0.057	0.065	0.056
99	19.015	18.739	18.673	18.494	18.342	18.363	18.321	18.171	17.915	17.816	17.880	17.670
	0.204	0.185	0.167	0.179	0.146	0.181	0.226	0.199	0.167	0.145	0.192	0.164
100	17.161	17.057	17.137	17.160	17.172	17.307	17.342	17.371	17.529	17.575	17.569	17.901
	0.036	0.039	0.043	0.052	0.049	0.059	0.099	0.085	0.113	0.120	0.141	0.207
101	19.580	19.227	19.624	19.130	19.019	19.071	19.863	19.110	19.108	18.962	19.296	19.319
	0.414	0.344	0.431	0.343	0.282	0.326	0.899	0.448	0.524	0.442	0.677	0.715
103	19.482	19.223	19.071	18.870	18.764	18.713	19.007	18.876	19.205	18.948	18.872	19.680
	0.354	0.321	0.257	0.259	0.218	0.225	0.418	0.333	0.528	0.422	0.438	0.945
107	18.788	18.541	18.507	18.462	18.378	18.395	18.229	18.273	18.119	18.037	18.070	18.003
	0.070	0.059	0.049	0.060	0.044	0.049	0.053	0.058	0.059	0.061	0.084	0.084

Table 2: Continued

No.	03	04	05	06	07	08	09	10	11	12	13	14
(1)	(2)	(3)	(4)	(5)	(6)	(7)	(8)	(9)	(10)	(11)	(12)	(13)
113	19.868	19.545	19.527	19.685	19.362	19.618	19.706	19.577	19.689	19.498	19.968	20.229
	0.109	0.074	0.068	0.089	0.066	0.083	0.101	0.122	0.146	0.142	0.324	0.438
115	17.867	17.660	17.796	17.740	17.836	17.857	17.920	17.798	17.940	17.874	17.975	17.971
	0.023	0.018	0.018	0.020	0.019	0.023	0.027	0.029	0.038	0.039	0.055	0.063
117	19.060	18.904	18.837	18.710	18.726	18.790	18.718	18.741	18.765	18.636	18.809	18.355
	0.164	0.160	0.132	0.149	0.156	0.177	0.196	0.213	0.252	0.228	0.362	0.253
118	18.322	18.002	17.883	17.658	17.515	17.387	17.274	17.129	17.049	17.104	16.974	16.722
	0.163	0.154	0.123	0.126	0.091	0.094	0.087	0.084	0.084	0.084	0.089	0.066
119	18.481	18.162	18.088	17.866	17.719	17.599	17.540	17.336	17.262	17.306	17.163	16.898
	0.160	0.154	0.122	0.126	0.093	0.094	0.096	0.082	0.086	0.081	0.086	0.063
120	18.281	17.983	18.108	18.002	18.041	18.003	18.165	18.019	18.252	18.369	18.309	19.015
	0.261	0.236	0.234	0.280	0.234	0.276	0.309	0.308	0.427	0.429	0.470	0.904
121	18.602	18.290	18.297	18.184	18.466	18.422	17.962	18.808	19.161	19.213	19.548	19.123
	0.189	0.148	0.139	0.137	0.147	0.154	0.189	0.221	0.370	0.412	0.739	0.600
122	17.297	17.137	17.189	17.132	17.025	17.054	17.125	17.010	17.031	16.954	16.881	16.804
	0.165	0.145	0.129	0.144	0.096	0.123	0.200	0.155	0.186	0.134	0.146	0.135
124	18.820	18.849	19.003	18.906	19.068	19.208	19.177	19.057	18.998	19.262	19.231	19.251
	0.144	0.161	0.155	0.173	0.163	0.208	0.218	0.194	0.189	0.276	0.293	0.324
125	18.412	18.348	18.463	18.429	18.485	18.500	18.520	18.491	18.812	18.746	18.457	18.364
	0.134	0.157	0.160	0.192	0.183	0.220	0.258	0.273	0.423	0.368	0.309	0.277
126	20.649	19.648	19.545	19.327	18.988	18.935	19.072	18.551	18.416	18.252	18.116	17.992
	0.876	0.393	0.362	0.366	0.223	0.235	0.312	0.190	0.188	0.151	0.153	0.146
127	15.712	15.650	15.796	15.767	15.971	15.950	15.990	15.966	15.994	16.108	16.167	16.250
	0.035	0.037	0.038	0.044	0.065	0.070	0.104	0.095	0.104	0.107	0.126	0.139
128	18.885	18.545	18.441	18.464	18.246	18.375	18.286	18.155	17.886	17.819	17.829	17.690
	0.429	0.352	0.268	0.367	0.263	0.342	0.327	0.330	0.298	0.268	0.291	0.281
129	18.234	18.107	18.174	18.193	17.865	18.039	18.037	17.910	17.675	17.642	17.357	17.286
	0.204	0.214	0.203	0.280	0.159	0.235	0.276	0.261	0.236	0.213	0.167	0.177

Table 2: Continued

No.	03	04	05	06	07	08	09	10	11	12	13	14
(1)	(2)	(3)	(4)	(5)	(6)	(7)	(8)	(9)	(10)	(11)	(12)	(13)
135	19.484	19.079	19.000	19.412	19.010	18.905	18.500	18.947	18.643	18.708	18.632	18.785
	0.355	0.290	0.226	0.425	0.236	0.220	0.153	0.258	0.188	0.248	0.261	0.356
136	19.374	19.079	19.099	18.960	18.877	18.905	18.869	18.865	18.835	18.719	18.731	18.949
	0.213	0.216	0.201	0.236	0.187	0.224	0.205	0.242	0.258	0.221	0.275	0.342
137	18.374	18.095	18.196	18.136	18.121	18.130	18.066	18.137	18.138	18.090	18.139	17.906
	0.072	0.065	0.067	0.074	0.064	0.075	0.082	0.090	0.103	0.101	0.140	0.106
139	18.633	18.520	18.578	18.535	18.458	18.413	18.351	18.317	18.227	18.332	18.352	17.962
	0.069	0.062	0.063	0.066	0.056	0.061	0.067	0.069	0.072	0.082	0.116	0.079
141	16.069	15.987	16.128	16.155	16.240	16.306	16.371	16.357	16.419	16.395	16.284	16.346
	0.033	0.043	0.041	0.051	0.041	0.052	0.078	0.064	0.075	0.067	0.071	0.071
142	15.743	15.699	15.809	15.800	15.863	15.856	15.761	15.617	15.451	15.305	15.310	15.184
	0.012	0.011	0.010	0.014	0.010	0.011	0.012	0.010	0.009	0.007	0.009	0.008
144	19.991	19.810	19.717	19.464	19.386	19.214	18.917	19.089	19.036	19.060	19.145	19.179
	0.280	0.216	0.187	0.175	0.124	0.123	0.125	0.143	0.130	0.126	0.239	0.206
145	20.109	19.798	19.680	19.592	19.385	19.249	19.422	19.360	19.483	19.586	19.931	19.743
	0.255	0.202	0.169	0.188	0.136	0.141	0.179	0.192	0.238	0.285	0.452	0.431
146	18.574	18.249	18.294	18.135	18.350	18.303	18.350	18.470	18.363	18.436	18.446	18.493
	0.278	0.245	0.235	0.272	0.246	0.273	0.393	0.357	0.387	0.358	0.432	0.426
147	18.439	18.360	18.441	18.356	18.420	18.419	18.328	18.393	18.521	18.541	18.809	18.709
	0.033	0.031	0.027	0.027	0.026	0.033	0.031	0.042	0.046	0.060	0.134	0.100
148	18.016	17.901	17.520	18.051	18.136	18.184	17.009	18.122	18.111	18.200	18.618	17.935
	0.076	0.072	0.041	0.068	0.072	0.081	0.040	0.108	0.119	0.130	0.238	0.134
150	17.541	17.380	17.432	17.361	17.408	17.432	17.426	17.410	17.444	17.470	17.575	17.479
	0.064	0.062	0.053	0.070	0.067	0.079	0.085	0.093	0.104	0.101	0.128	0.119
151	17.717	17.493	17.502	17.390	17.333	17.305	17.257	17.200	17.152	17.097	17.067	16.968
	0.063	0.063	0.055	0.067	0.054	0.061	0.062	0.062	0.064	0.059	0.068	0.063
152	19.190	18.928	18.904	18.942	18.840	18.901	18.746	18.870	18.701	18.730	18.806	18.683
	0.137	0.130	0.128	0.156	0.125	0.148	0.145	0.177	0.163	0.171	0.249	0.206

Table 2: Continued

No.	03	04	05	06	07	08	09	10	11	12	13	14
(1)	(2)	(3)	(4)	(5)	(6)	(7)	(8)	(9)	(10)	(11)	(12)	(13)
157	20.023	19.557	19.483	19.239	19.180	19.180	19.181	19.103	19.149	19.052	19.202	19.499
	0.401	0.310	0.247	0.264	0.210	0.229	0.258	0.247	0.303	0.266	0.370	0.532
158	15.950	15.913	15.947	16.070	16.158	16.146	15.869	16.074	15.849	15.869	15.813	15.508
	0.044	0.050	0.045	0.065	0.051	0.058	0.057	0.059	0.055	0.048	0.054	0.043
159	16.699	16.684	16.909	16.777	17.034	16.943	16.937	16.984	16.903	17.134	16.907	16.910
	0.034	0.032	0.035	0.036	0.035	0.036	0.056	0.049	0.052	0.056	0.063	0.064
160	18.762	18.558	18.638	18.565	18.521	18.452	18.495	18.332	18.366	18.334	18.042	18.183
	0.098	0.088	0.082	0.091	0.072	0.079	0.098	0.082	0.090	0.091	0.110	0.119
161	19.364	19.028	18.869	18.660	18.457	18.339	18.180	18.074	17.956	17.942	17.951	17.631
	0.077	0.054	0.039	0.034	0.033	0.033	0.034	0.036	0.035	0.038	0.059	0.043
162	20.196	20.274	20.054	19.939	19.828	19.798	19.283	19.342	19.375	19.258	19.030	19.141
	0.130	0.106	0.095	0.089	0.078	0.087	0.097	0.080	0.089	0.087	0.143	0.135

Table 3: Comparison of Cluster Photometry with Previous Measurements

No.	V (Chandar et al.)	V (BATC)	No.	V (Chandar et al.)	V (BATC)
(1)	(2)	(3)	(1)	(2)	(3)
62.....	18.769 ± 0.005	19.332 ± 0.240	108.....	19.162 ± 0.006	19.262 ± 0.216
64.....	19.007 ± 0.008	19.107 ± 0.147	109.....	18.527 ± 0.000	17.802 ± 0.079
67.....	17.446 ± 0.002	17.515 ± 0.056	110.....	18.515 ± 0.003	18.596 ± 0.078
68.....	17.963 ± 0.003	17.953 ± 0.082	112.....	18.625 ± 0.004	18.580 ± 0.091
69.....	18.541 ± 0.005	18.697 ± 0.179	113.....	19.269 ± 0.006	19.443 ± 0.122
71.....	18.822 ± 0.004	19.134 ± 0.183	115.....	19.648 ± 0.007	17.857 ± 0.033
72.....	18.321 ± 0.003	18.293 ± 0.089	117.....	18.363 ± 0.006	18.759 ± 0.261
73.....	19.430 ± 0.007	19.536 ± 0.183	118.....	17.945 ± 0.005	17.662 ± 0.162
74.....	18.780 ± 0.003	18.827 ± 0.119	119.....	18.247 ± 0.006	17.864 ± 0.164
75.....	19.534 ± 0.007	19.105 ± 0.256	120.....	18.169 ± 0.000	18.100 ± 0.414
76.....	19.687 ± 0.000	18.961 ± 0.196	121.....	18.431 ± 0.010	18.448 ± 0.241
77.....	18.778 ± 0.003	18.153 ± 0.059	122.....	17.343 ± 0.004	17.109 ± 0.182
78.....	18.238 ± 0.003	18.221 ± 0.125	124.....	18.859 ± 0.009	19.029 ± 0.286
79.....	18.969 ± 0.005	18.945 ± 0.210	125.....	17.983 ± 0.005	18.521 ± 0.316
83.....	19.426 ± 0.006	19.593 ± 0.159	126.....	18.518 ± 0.007	19.174 ± 0.417
84.....	19.705 ± 0.006	20.023 ± 0.247	127.....	16.394 ± 0.003	15.971 ± 0.102
86.....	18.945 ± 0.004	19.158 ± 0.097	128.....	17.841 ± 0.010	18.334 ± 0.492
87.....	19.041 ± 0.006	19.037 ± 0.080	129.....	17.383 ± 0.006	17.974 ± 0.325
88.....	18.198 ± 0.003	17.884 ± 0.248	130.....	17.838 ± 0.006	17.541 ± 0.142
89.....	18.538 ± 0.004	18.393 ± 0.269	131.....	18.262 ± 0.007	17.684 ± 0.095
91.....	17.886 ± 0.003	17.861 ± 0.075	132.....	18.678 ± 0.014	18.990 ± 0.292
92.....	18.605 ± 0.008	18.683 ± 0.171	133.....	18.106 ± 0.006	18.494 ± 0.213
93.....	19.105 ± 0.014	19.449 ± 0.350	135.....	18.826 ± 0.013	19.233 ± 0.445
94.....	18.478 ± 0.005	18.516 ± 0.109	136.....	18.807 ± 0.011	18.954 ± 0.336
95.....	18.289 ± 0.004	17.872 ± 0.065	137.....	18.011 ± 0.006	18.182 ± 0.112
96.....	19.075 ± 0.009	19.486 ± 0.312	139.....	18.223 ± 0.004	18.556 ± 0.097
97.....	18.283 ± 0.006	18.455 ± 0.117	141.....	16.281 ± 0.002	16.250 ± 0.074
99.....	18.154 ± 0.006	18.443 ± 0.262	142.....	15.854 ± 0.001	15.904 ± 0.018
100.....	17.697 ± 0.007	17.183 ± 0.085	144.....	19.055 ± 0.014	19.526 ± 0.220
101.....	18.721 ± 0.012	19.097 ± 0.498	145.....	19.329 ± 0.016	19.555 ± 0.242
103.....	18.525 ± 0.011	18.874 ± 0.374	146.....	18.577 ± 0.012	18.355 ± 0.422
107.....	18.378 ± 0.003	18.459 ± 0.079	147.....	18.423 ± 0.007	18.459 ± 0.045

Table 3: Continued

No.	V (Chandar et al.)	V (BATC)	No.	V (Chandar et al.)	V (BATC)
(1)	(2)	(3)	(1)	(2)	(3)
148.....	17.714 ± 0.006	18.152 ± 0.120	156.....	18.341 ± 0.008	18.331 ± 0.177
150.....	17.398 ± 0.004	17.444 ± 0.115	157.....	18.979 ± 0.012	19.258 ± 0.369
151.....	17.242 ± 0.004	17.419 ± 0.095	158.....	16.191 ± 0.002	16.192 ± 0.091
152.....	18.632 ± 0.009	18.912 ± 0.223	159.....	17.000 ± 0.003	17.039 ± 0.058
153.....	18.610 ± 0.009	18.619 ± 0.176	160.....	18.458 ± 0.007	18.617 ± 0.127
154.....	17.924 ± 0.005	17.772 ± 0.070	161.....	18.749 ± 0.005	18.620 ± 0.055
155.....	17.504 ± 0.003	17.546 ± 0.055	162.....	19.920 ± 0.014	19.933 ± 0.135

Table 4: Age Distribution of 78 Star Clusters

No.	Metallicity (Z)	Age ([log yr])	No.	Metallicity (Z)	Age ([log yr])
(1)	(2)	(3)	(1)	(2)	(3)
62.....	0.00040	9.279	108.....	0.00400	8.507
64.....	0.00400	8.806	109.....	0.00040	8.657
67.....	0.00400	7.720	110.....	0.00040	8.957
68.....	0.00400	7.021	112.....	0.00040	9.207
69.....	0.00040	9.760	113.....	0.00040	7.806
71.....	0.02000	8.606	115.....	0.02000	6.840
72.....	0.02000	9.107	117.....	0.00400	8.009
73.....	0.02000	9.107	118.....	0.02000	9.155
74.....	0.00400	9.322	119.....	0.02000	9.155
75.....	0.00040	8.757	120.....	0.00400	6.600
76.....	0.00400	8.757	121.....	0.02000	6.620
77.....	0.02000	9.009	122.....	0.00400	8.307
78.....	0.02000	6.800	124.....	0.02000	6.860
79.....	0.02000	9.107	125.....	0.00400	6.860
83.....	0.02000	6.940	126.....	0.02000	9.954
84.....	0.02000	6.860	127.....	0.00040	7.220
86.....	0.00040	9.155	128.....	0.00400	9.107
87.....	0.00040	10.061	129.....	0.02000	6.940
88.....	0.00400	6.480	130.....	0.00400	9.057
89.....	0.00040	6.580	131.....	0.00040	9.301
91.....	0.00040	9.255	132.....	0.02000	6.980
92.....	0.00400	7.699	133.....	0.02000	6.960
93.....	0.00400	6.600	135.....	0.02000	6.940
94.....	0.00040	8.356	136.....	0.00040	8.806
95.....	0.02000	6.940	137.....	0.02000	8.057
96.....	0.02000	6.920	139.....	0.02000	7.179
97.....	0.00400	10.279	141.....	0.00040	6.660
99.....	0.02000	9.107	142.....	0.02000	6.940
100.....	0.02000	6.680	144.....	0.00040	9.107
101.....	0.02000	8.057	145.....	0.00040	8.009
103.....	0.00400	6.620	146.....	0.00040	8.009
107.....	0.00400	8.857	147.....	0.02000	6.760

Table 4: Continued

No.	Metallicity (Z)	Age ([log yr])	No.	Metallicity (Z)	Age ([log yr])
(1)	(2)	(3)	(1)	(2)	(3)
148.....	0.02000	6.840	156.....	0.00040	8.009
150.....	0.00040	8.009	157.....	0.00040	8.957
151.....	0.00400	8.757	158.....	0.02000	6.980
152.....	0.00400	8.356	159.....	0.00400	7.179
153.....	0.00040	8.906	160.....	0.00040	8.507
154.....	0.00040	8.507	161.....	0.02000	9.225
155.....	0.00400	6.960	162.....	0.00400	10.283

This figure "majunfig1.gif" is available in "gif" format from:

<http://arxiv.org/ps/astro-ph/0202363v1>